Wearable Belt Antenna for Body Communication Networks

Rui Pei, Mark Leach, Eng Gee Lim, Zhao Wang, Jingchen Wang, Yuanchen Wang, Zhenzhen Jiang, and Yi Huang

***Abstract*—This paper presents a dual-band wearable belt antenna design offering stable performance for both on and off body scenarios. The proposed antenna is composed of a metal buckle and a lossy leather substrate. A layer of conductive fiber is attached to the leather to provide isolation between the human body and the radiating element. A novel snap-on button structure is used as the antenna feed. The antenna can achieve an on body realized gain of 5.10 dBi at 2.45 GHz, 4.05 dBi at 5.2 GHz and 3.31 dBi at 5.8 GHz. A specific absorption rate of 0.87 W/kg is achieved. The on/off body radiation efficiency of the antenna is measured in a reverberation chamber. The antenna can operate in both on and off-body communication as the frequency shift induced by the human body tissue is not significant. The proposed belt antenna is a low-cost and reliable solution for smart on-body applications.**

***Index Terms*—Belt antenna, dual-band antenna, on/off body radiation pattern, wearable antenna.**

I. Introduction

The increasing popularity of wearable electronic devices has brought more attention to wearable antenna designs. Wearable antenna designs should address the following three challenges during the design process, frequency shifting and radiation distortion due to the proximity of the body tissues, Specific Absorption Rate (SAR) limitations and the ergonomics and robustness of the design. To contend with these challenges, previous studies have tried to exploit existing metal parts of personal accessories worn daily as the radiating element of the antenna. Examples of such designs include button antennas [1]-[4], watch strap antennas [5], watch frame antennas [6], zipper antennas [7], shoelace antennas and belt buckle antennas [8]-[10]. Each of these has restrictions in terms of their shape and size in order to maintain their function as wearable accessories.

The belt buckle is an ideal platform for wearable antenna designs due to its metallic nature and relatively large size. Previous studies [9]-[10] have used single tongue buckles (as shown in Fig. 1. (a) and (b)) as the main radiation element of the antenna proving the feasibility of the idea. However, the loop structure of these buckles would result in a radiation pattern similar to a one wavelength loop antenna, which is omnidirectional in the vertical plane. This radiation pattern would mean that a large portion of the radiation is directed towards the human body from the belt antenna, leading to low radiation efficiency and hence low realized gain. Tissue absorption would also raise concerns about SAR.

In this paper, a dual-band belt antenna based on a pin buckle, as shown in Fig. 1. (c) and (d), is proposed. For this type of belt, there is a pin on the back of the buckle, which hooks through one of the notches in the belt leather to hold the belt in position. In the proposed design, the buckle and the pin function as the radiating element. In addition, a layer of conductive fiber is attached to the leather to provide isolation to the human body. A snap-on button structure is used as the feed point as well as to hold the pin stable during use. Despite being quite lossy (a loss tangent of 0.08), leather is chosen to be the main material for the belt due to its popularity in the market.

The proposed antenna operates over bands around 2.4 GHz and 5 GHz. It has stable performance in both on-body and off-body situations. Without using any specific low loss materials for radio frequency applications, the designed antenna achieves desirable levels of on body radiation efficiency and realized gain.

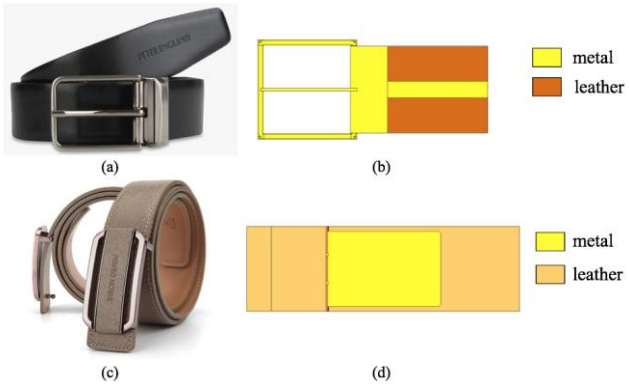

Fig. 1. Types of belt buckle and corresponding antenna design. (a) Single tongue buckle [11]. (b) Single tongue antenna design as in [9] and [10]. (c) Pin buckle [11]. (d) Pin buckle antenna design proposed in this study.

The remainder of this paper is organized as follows. In section II, the proposed antenna geometry and key parameters will be discussed. In section III, the effect of the human body on the antenna performance is analyzed using a variety of human voxel models. The fabricated antenna and measurement results are presented in section IV. Section V provides conclusions drawn from this study.

II. Antenna Topology

A. Key parameters of the antenna design

The key parameters of this antenna design are illustrated with Fig. 2, with specific parameter values listed in TABLE I. The metallic buckle and pin for this design are made of brass. The snap-on button used here is a commercial one made of stainless steel. The ground layer is a conductive fiber glued to the leather. The conductive fiber is produced by the YGM company located in Foshan, China. The relative dielectric constant of the leather was measured to be 2.9 and the loss tangent was measured to be 0.08. The measurements were performed using Keysight N1501A dielectric probe kit.

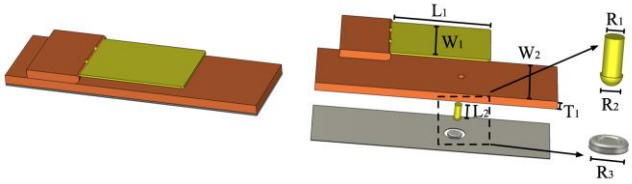

Fig. 2. The structure of the proposed belt antenna and key parameters

Manuscript received XX, 2020; revised XX; accepted XX. Date of publication XX; date of current version XX. This work was partially supported by the XJTLU Research Development Fund (PGRS-13-03-06, RDF-14-03-24 and RDF-14-02-48) and AI University Research Centre (AI-URC) through Key Programme Special Fund (KSF-P-02). (*Corresponding author: Mark Leach.*)

R. Pei, M. Leach, E. G. Lim, Z. Wang, J. Wang, Y. Wang and Z. Jiang are with the Department of Electrical and Electronics Engineering, Xi'an Jiaotong Liverpool University, Suzhou 215123, China.

Y. Huang is with the Department of Electrical Engineering and Electronics, University of Liverpool, Liverpool L69 3BX, U.K.

Digital Object Identifier 10.1109/LAWP.2019.xxx

TABLE I
ANTENNA GEOMETRY PARAMETERS

Symbol	Quantity	Value (mm)
W_1	width of the metal cap	25
W_2	width of the belt leather	30
L_1	length of the metal cap	42
L_2	length of the belt pin	7.7
R_1	radius of the belt pin	3
R_2	radius of the belt pin snap-on	3.5
R_3	radius of the snap-on button	6
T_1	thickness of the leather	3.6

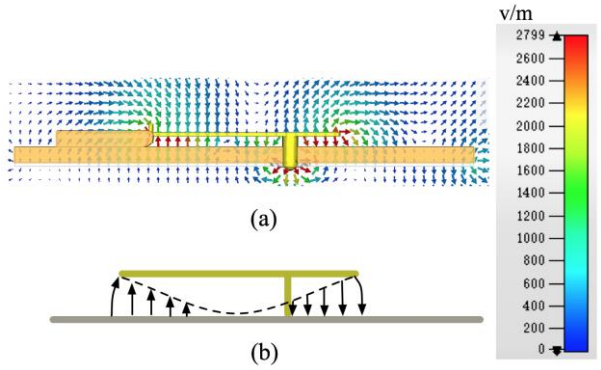

Fig. 3. The E-field distribution of the proposed belt buckle at 2.45 GHz. (a) The simulated E-field distribution. (b) A sketch of the operation mechanism: a TM_{10} mode.

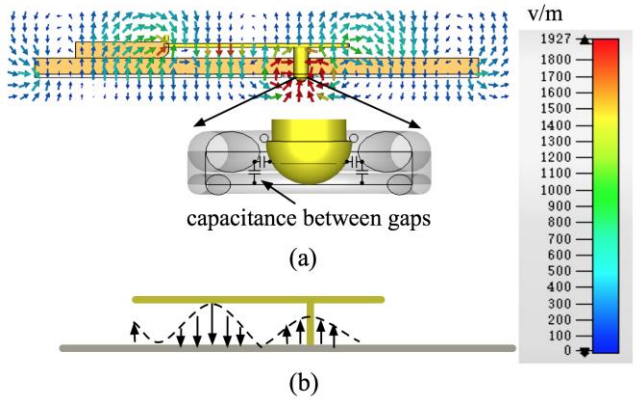

Fig. 4. The E-field distribution of the proposed belt buckle at 5.5 GHz. (a) The simulated E-field distribution with the snap-on button structure enlarged. (b) A sketch of the operation mechanism: a quasi-TM_{30} mode.

B The design strategy and the working principle.

At 2.45 GHz, the proposed belt antenna functions as an elevated patch antenna with a TM_{10} mode. The E-field distribution and a sketch of the TM_{10} mode are included in Fig. 3. The 2D field cross-section was taken at the position of the feeding pin to illustrate the effect of the pin on the electrical field distribution. In Fig. 3. (a), a strong E-field distribution can be seen beneath the snap-on button, where the maximal SAR value was observed in the following voxel human body analysis. There are two reasons why the patch was designed to be elevated. The first is that the leather material selected in this design, which is widely used in belt manufacture, has a relatively large loss tangent. The slight elevation was found to reduce the loss and hence increase radiation efficiency. The second is that the presence of this small gap is common among pin buckle belts. In a number of belt designs studied during the research, the tip of the pin would hook to the leather and leave a gap between the metal cap and the leather. This is an ergonomic design and allows the buckle to accommodate belt leathers with slightly different thicknesses and curvatures. The locking mechanism of the snap-on button structure endured the size of the gap while the belt antenna is in use on the human body. In the 5 GHz band, the radiation follows a quasi-TM_{30} principle. The E-field distribution at 5.5 GHz is shown in Fig. 4 (a) along with a magnified structure of the connection between the snap-on button and the belt pin. The cavity between the tip of the pin and the button creates parallel capacitance which compensates for the inductance brought about by the long feeding pin. The size of the snap-on button was carefully selected for impedance matching. The E-field distribution near the feeding pin does not coincide with the conventional TM_{30} mode as a transverse electrical field is present. Nonetheless, the field distribution elsewhere, especially at the radiation edge, still coincides with that of a TM_{30} mode.

The ground plane was made of conductive fiber adhered to the back of the leather. It provided enough isolation between the radiating elements and the human body to achieve a low SAR value. A small gap is left between the conductive ground and the bottom of the snap-on button to place the feed.

III. THE EFFECT OF THE HUMAN BODY

The belt antenna will function in close proximity to the human body and thus the effect of body tissues must be evaluated. The model Gustav (38-year-old male, 176 cm and 69 kg) from the CST voxel family was used to evaluate the effect of the human body on the antenna performance. Two common postures, standing straight and sitting down were customized with CST poser and used in the analysis.

A. The effect of the standing/sitting human body.

The effect of the human body on the belt antenna performance includes the following two aspects: frequency shifting due to the dielectric properties of the body tissue nearby and the reflection/absorption of the overall human body. The simulated and measured *S* parameters with the two human body postures are summarized in Fig 5. With the isolation provided by the textile ground layer, the frequency shift due to the human body tissue is not significant. The bandwidths for each posture with a -10 dB criterion are listed in TABLE II. In terms of the reflection coefficient, the proposed antenna can achieve both on-body and off-body communication. In the 5 GHz band, a higher level of absorption can be seen in the sitting case, in both simulation and measurement results. The main absorption in this case happens at the upper thigh.

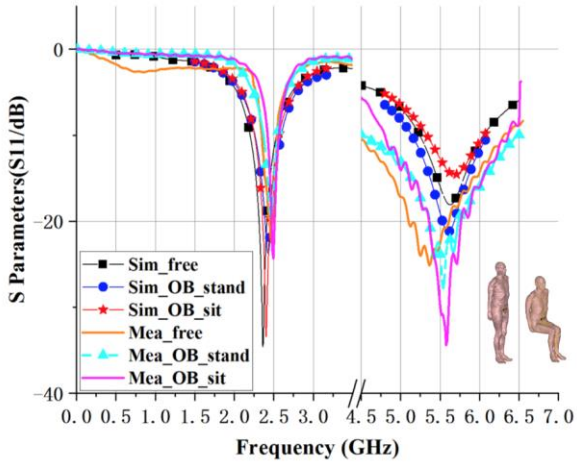

Fig. 5. Simulated and measured S_{11} (OB: on body).

B. The effect of body build and shape.

Different body shapes present different material compositions. In terms of electromagnetics, this means that the dielectric properties close to the antenna are person dependent. Two additional CST voxel models have been used to analyse the performance of the antenna in this work as follows: Donna (40-year-old female, 176 cm, 79 kg, standing) and Child (7-year-old female, 115 cm, 21.7 kg, standing).

The results with different voxel models are summarized in TABLE II. The proposed belt antenna achieves relatively stable performance in terms of both bandwidth and radiation pattern across the family of human body models.

Moreover, antenna performance under various bending conditions has been studied. As shown in Fig. 6, the antenna was bended towards cylinders with radius of 200 mm and 250 mm in simulation. Such level of bending is more severe than the antenna would experience on actual human body. A frequency shift can be seen as the result of the bending. For on-body measurements, the antenna was attached tightly to the human body to experience the actual level of bending. In both cases, the antenna performance can be considered stable and fit for the application.

TABLE II

SIMULATED ANTENNA PERFORMANCE WITH DIFFERENT VOXEL MODEL

Model.	BW(GHz)/%	Realized Gain dBi at 2.45/5.2/5.8 (GHz)
Free space	2.19-2.52/13.4% 5.23-6.05/14.9%	4.59/1.73/0.92
Gustav stand	2.26-2.58/13.0% 5.14-6.1/17.4%	5.31/4.21/3.52
Gustav sit	2.25-2.56/12.6% 5.31-6.06/13.6%	6.54/5.33/4.74
Donna	2.28-2.57/11.8% 5.15-6.08/16.9%	4.97/3.91/3.37
Child	2.27-2.60/13.4% 5.22-6.06/15.2%	4.81/3.99/3.28

TABLE III

COMPARISON OF ANTENNA PERFORMANCE WITH OTHER SYSTEMS

Ref.	BW(GHz)/%	Realized Gain (dBi)	SAR (10g)
[3] (button)	2.38-2.52/6% 4.92-6.9/36%	0.24 (2.45 GHz) 4.73 (5.2 GHz) 4.29 (5.8 GHz)	0.18 (2.45 GHz) 0.12 (5.2 GHz) 0.13 (5.8 GHz)
[6] (watch)	2.33-2.60/11%	-0.89 (2.45 GHz)	N/A
[7] (zipper)	2.37-2.49/4.92%	5 (2.45 GHz)	N/A
[8] (shoelace)	2.43(center)/11%	9.73 (2.45 GHz)	N/A
[9] (belt)	2.45 (center)/22.8% 5.25 (center)/9.4%	2.8 (2.45 GHz) 4.5 (5.25 GHz)	N/A
[10] (belt)	0.7-1.2/55.56% 1.69-2.63/38.37%	-4.16 (0.9 GHz) -8.61 (1.8 GHz) -8.61 (2.45 GHz)	1.90 (0.9 GHz) 1.63 (1.8 GHz) 1.00 (2.45 GHz)
Proposed	2.28-2.53/10.2% 4.88-6.15/23.1%	5.10 (2.45 GHz) 4.05 (5.2 GHz) 3.31 (5.8 GHz)	0.87 (2.45 GHz) 0.83 (5.2 GHz) 0.13 (5.8 GHz)

IV. THE RESULTS AND MEASUREMENTS

The proposed belt antenna was fabricated and tested. For ease of production, the metal structure was 3D printed with brass. The resulting belt prototype is shown in Fig. 7 (a). The off-body radiation pattern of the belt antenna was measured in an anechoic chamber as shown in Fig. 7 (b). A holder with similar curvature of the human waist was 3D printed for the test.

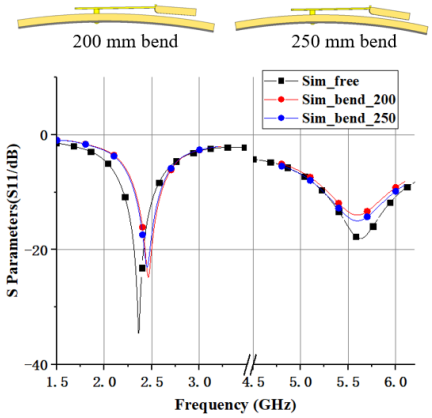

Fig. 6. The simulated S11 of the belt antenna for 3 cases: free space, bending towards cylinders with radius of 200 mm and 250 mm.

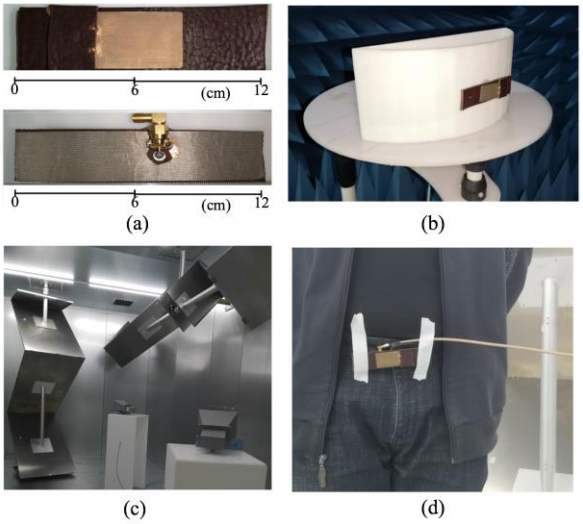

Fig. 7. (a) Belt antenna prototype (b) Anechoic chamber measurement (c) Reverberation chamber measurement. (d) On-body measurement in a reverberation chamber.

A. The bandwidth and the radiation pattern.

The measured S_{11} is included in Fig. 5 for comparison. A frequency shift can be observed with human presence in both simulation and measurement. A discrepancy can be found for the sitting case between simulated and measured results. This is mainly due to the upper thigh of the human body which was located close to the main beam in the sitting case. In our on-body measurement, the test subject had trousers on and the biological composition of the test subject was different from the voxel data applied during simulation. A reduction in bandwidth in the 2.45 GHz band in the on-body cases can be seen in Fig. 5. This is likely due to the bending of the cable when placing the belt antenna close to the actual human body.

The measured radiation patterns are shown in Fig 8 along with the simulated results with/without human voxel data. The simulated front-to-back ratio in free space is 8.275 dB at 2.45 GHz, 8.80 dB at

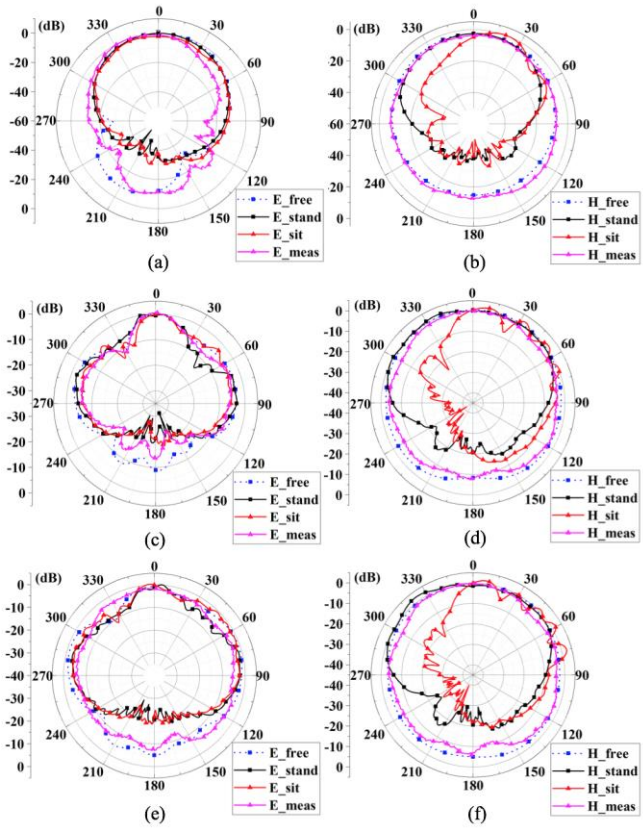

Fig. 8. Simulated and measured radiation patterns: (a) E-plane at 2.45 GHz. (b) H-plane at 2.45 GHz. (c) E-plane at 5.2 GHz. (d) H-plane at 5.2 GHz. (e) E-plane at 5.8 GHz. (f) H-plane at 5.8 GHz.

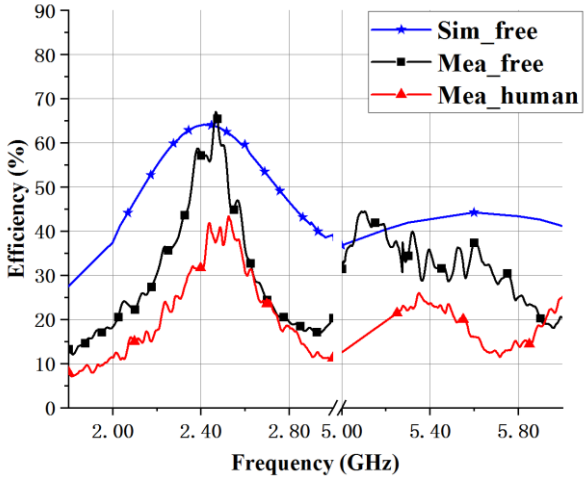

Fig. 9. Simulated and measured radiation efficiency

5.2 GHz and 4.99 dB at 5.8 GHz. The measured front-to-back ratio is 9.128 dB at 2.45 GHz, 13.31 dB at 5.2 GHz and 7.09 dB at 5.8 GHz, respectively. Due to the presence of the antenna holder in the anechoic chamber, the measured values were higher than the simulated ones. Generally, the measured results match the simulation results well.

B. The measurement of on body realized gain & radiation efficiency.

The on-body realized gain was measured in our in-house anechoic chamber with a test subject (male, 188 cm and 82 kg). The antenna was attached to the waist of the test subject with the subject standing straight during the measurement. The measured results were summarized in TABLE III. A comparison with other state-of-the-art wearable solutions was also included in TABLE III. It should be noted that due to the lack of original performance data, the reference [10] listed was remodeled and re-simulated in the same simulation environment as this work and the data here was the simulation result.

The on-body efficiency, which is an important parameter for wearable antenna applications, was also studied with the same human subject. An in-house reverberation chamber (length: 5.4 m, width: 3.0 m, height: 2.8 m), as shown in Fig. 7 (c), was used to enclose both the human subject and the proposed belt antenna. The chamber has one vertical and one horizontal stirrer. The lowest usable frequency (LUF) of the chamber is 300 MHz. For on-body measurement, the belt antenna was fixed at the waist of the test subject, as shown in Fig. 7 (d). The measurement of the on-body efficiency follows the method presented in [15]. The human subject would have a severe loading effect on the chamber. Thus, calibration with the human subject in the chamber is required prior to measurement. During each measurement, the dressing of the test subject was kept constant, including the contents in the subject's pockets. The stirring sequence in this experiment included mechanical stirring (2 degrees, 180 measurements), polarization stirring (two orthogonal linear polarizations) and position stirring (4 receiver positions). A total of 1440 measured sample points were taken for each frequency point. A large number of samples were required to keep the uncertainty of the measurement to an acceptable level. Meanwhile, the number of mechanical stirs in each run was limited so that the test subject did not have to stay in the chamber for a prolonged amount period of time. The receiving antenna in the chamber was spaced by a half-wavelength for each run to create independent samples. The resulting radiation efficiency is shown in Fig 9. In both frequency bands, an efficiency degradation of approximately 20% can be seen when the belt antenna is closely attached to the human subject.

V. Conclusion

In this study, a dual-band belt antenna based on the pin buckle belt was proposed. Without using any dedicated low-loss substrates for RF applications, the antenna was still able to achieve an on-body realized gain of 5.10 dBi and a radiation efficiency of approximately 40 % at 2.45 GHz. A snap-on button and pin structure was used as the feeding structure. This structure provided a sufficient level of fixture for the antenna to have a stable on-body performance. A TM_{10} mode and a quasi-TM_{30} mode similar to a microstrip patch antenna were applied for the two resonance frequencies. Unlike a conventional loop-based belt buckle structure, this design limits the radiation towards the inside of the human body and ensures that the specific absorption rate in both bands was well within standard safety limits [13]-[14]. This design also ensured a relatively high level of on-body radiation efficiency, which was measured in a reverberation chamber. The belt antenna maintains stable performance for both on and off-body communication. It is a low-cost, highly-efficient and reliable solution for wearable body area network applications.

Acknowledgment

The authors would like to thank CST AG for providing the CST STUDIO SUITE Electromagnetic Simulation Software package under the China Key University Promotion Program and Suzhou Municipal

Key Lab for Wireless Broadband Access Technologies in the Department of Electrical Engineering, Xi'an Jiaotong Liverpool Univ, for research facilities.

REFERENCES

[1] X. Y. Zhang, H. Wong, T. Mo, and Y. F. Cao, "Dual-Band Dual-Mode Button Antenna for On-Body and Off-Body Communications," *IEEE Trans. on Biomed. Circuits Sys.*, vol. 11, pp. 933-941, 2017.

[2] H. Xiaomu, S. Yan, and G. A. E. Vandenbosch, "Wearable Button Antenna for Dual-Band WLAN Applications With Combined on and off-Body Radiation Patterns," *IEEE Trans. Antennas Propag.*, vol. 65, pp. 1384-1387, 2017.

[3] B. Sanz-Izquierdo, J. C. Batchelor, and M. I. Sobhy, "Button antenna on textiles for wireless local area network on body applications," *IET Microwaves, Antennas & Propagation*, vol. 4, pp. 1980-1987, 2010.

[4] S. J. Chen, T. Kaufmann, D. C. Ranasinghe, and C. Fumeaux, "A Modular Textile Antenna Design Using Snap-on Buttons for Wearable Applications," *IEEE Trans. Antennas Propag.*, vol. 64, pp. 894-903, 2016.

[5] G. Li, G. Gao, J. Bao, B. Yi, C. Song, and L. Bian, "A Watch Strap Antenna for the Applications of Wearable Systems," *IEEE Access*, vol. 5, pp. 10332-10338, 2017.

[6] S. Su and Y. Hsieh, "Integrated Metal-Frame Antenna for Smartwatch Wearable Device," *IEEE Trans. Antennas Propag.*, vol. 63, pp. 3301-3305, 2015.

[7] G. Li, Y. Huang, G. Gao, X. Wei, Z. Tian, and L. Bian, "A Handbag Zipper Antenna for the Applications of Body-Centric Wireless Communications and Internet of Things," *IEEE Trans. Antennas Propag.*, vol. 65, pp. 5137-5146, 2017.

[8] G. Li, Z. Tian, G. Gao, L. Zhang, M. Fu, and Y. Chen, "A Shoelace Antenna for the Application of Collision Avoidance for the Blind Person," *IEEE Trans. Antennas Propag.*, vol. 65, pp. 4941-4946, 2017.

[9] B. Sanz-Izquierdo and J. C. Batchelor, "A Dual Band Belt Antenna," in *2008 International Workshop on Antenna Technology: Small Antennas and Novel Metamaterials*, pp. 374-377, 2008.

[10] D. Gaspar and A. A. Moreira, "Belt antenna for wearable applications," in *2009 IEEE Antennas and Propagation Society International Symposium*, pp. 1-4, 2009.

[11] Hiren. (2017). *23 Types of Belt Buckle to Play Everyday's Style Game Perfectly*. Available: https://www.looksgud.in/blog/types-of-belt-buckle-design-men/

[12] I. Guideline, "Guidelines for limiting exposure to time-varying electric, magnetic, and electromagnetic fields (up to 300 GHz)," *Health phys*, vol. 74, pp. 494-522, 1998.

[13] C. a. G. Affairs. (2016). *Specific absorption rate (SAR) for cellular telephones*. Available: https://www.fcc.gov/general/specific-absorption-rate-sar-cellular-telephones

[14] R. E. Fields, "Evaluating compliance with FCC guidelines for human exposure to radiofrequency electromagnetic fields," *OET bulletin*, vol. 65, pp. 1-52,1997.

[15] S. J. Boyes, P. J. Soh, Y. Huang, G. A. E. Vandenbosch, and N. Khiabani, "Measurement and Performance of Textile Antenna Efficiency on a Human Body in a Reverberation Chamber," *IEEE Trans. Antennas Propag.*, vol. 61, pp. 871-881, 2013.